

This article was downloaded by:

On: 22 January 2011

Access details: *Access Details: Free Access*

Publisher *Taylor & Francis*

Informa Ltd Registered in England and Wales Registered Number: 1072954 Registered office: Mortimer House, 37-41 Mortimer Street, London W1T 3JH, UK



The Journal of Adhesion

Publication details, including instructions for authors and subscription information:

<http://www.informaworld.com/smpp/title~content=t713453635>

Fatigue Crack Propagation at Polymer Adhesive Interfaces

J. E. Bitter^a; T. J. Lardner^a; W. Grayeski^a; G. C. Prakash^a; J. Lawrence^a

^a Mechanical and Industrial Engineering, University of Massachusetts, Amherst, MA, USA

To cite this Article Bitter, J. E. , Lardner, T. J. , Grayeski, W. , Prakash, G. C. and Lawrence, J.(1997) 'Fatigue Crack Propagation at Polymer Adhesive Interfaces', *The Journal of Adhesion*, 63: 4, 265 – 284

To link to this Article: DOI: 10.1080/00218469708017223

URL: <http://dx.doi.org/10.1080/00218469708017223>

PLEASE SCROLL DOWN FOR ARTICLE

Full terms and conditions of use: <http://www.informaworld.com/terms-and-conditions-of-access.pdf>

This article may be used for research, teaching and private study purposes. Any substantial or systematic reproduction, re-distribution, re-selling, loan or sub-licensing, systematic supply or distribution in any form to anyone is expressly forbidden.

The publisher does not give any warranty express or implied or make any representation that the contents will be complete or accurate or up to date. The accuracy of any instructions, formulae and drug doses should be independently verified with primary sources. The publisher shall not be liable for any loss, actions, claims, proceedings, demand or costs or damages whatsoever or howsoever caused arising directly or indirectly in connection with or arising out of the use of this material.

Fatigue Crack Propagation at Polymer Adhesive Interfaces

J. E. RITTER, T. J. LARDNER, W. GRAYESKI,
G. C. PRAKASH and J. LAWRENCE

*Mechanical and Industrial Engineering, University of Massachusetts,
Amherst, MA 01003, USA*

(Received 13 July 1996; In final form 9 October 1996)

Fatigue (slow) crack growth in epoxy/glass, epoxy acrylate/glass and epoxy/PMMA interfaces was studied under constant and cyclic loading at both high and low humidities using the interfacial, four-point flexure test. Finite element analysis was used to determine the energy release rate and phase angle appropriate for the different crack geometries observed. The experimental results show that for the polymer/glass interfaces, the primary driving force for fatigue crack growth is the applied energy release rate at the crack tip and that increasing test humidity enhances crack growth under constant loading but has an insignificant effect under cyclic loading. At low humidity the crack growth rates under cyclic loading are significantly greater than under constant loading. For epoxy/PMMA interfaces the crack growth results were independent of the applied energy release rate, relative humidity, and cyclic vs. constant loading, within experimental scatter. In addition, for polymer/glass interfaces the effect of phase angle (13 to 54°) on crack growth rates is not significant. However, for epoxy/PMMA interfaces the applied energy release rate for the initiation of crack growth is considerably greater for a phase angle of 66° than for 5°, indicating that increasing shear at the crack tip makes the initiation of crack growth more difficult. These results are discussed in terms of possible mechanisms of fatigue crack growth at polymer adhesive interfaces.

Keywords: Polymer adhesion; epoxy/glass; epoxy/PMMA; fatigue crack propagation; delamination; fracture toughness

INTRODUCTION

The understanding of interfacial delamination is critical for the successful use of polymer adhesives. Delamination of polymer adhesive interfaces is often characterized in terms of the fracture toughness of the interface as defined by the critical energy release rate (G_c) [1-4].

This characterization, however, is not sufficient since delamination often occurs at energy release rates (G) considerably below the critical G_c due to slow crack growth. Slow crack growth (generally known as fatigue) can occur due to cyclic loading [5,6] or to moisture-assisted crack growth under constant loading [7,8,9]. This previous research showed that for high humidities fatigue crack growth rates at epoxy acrylate/glass and epoxy/glass interfaces under constant loading are independent of crack geometry (phase angles from 13 to 54°) and are almost two orders of magnitude faster at high humidity than at low humidity. In addition, at low humidities crack growth rates at epoxy acrylate/glass interfaces under cyclic loading are significantly greater than under constant loading at the $G = G_{\max}$ of the cyclic loading.

The purpose of the present research is to expand our previous research on fatigue crack growth at epoxy acrylate/glass interfaces to include epoxy/glass and epoxy/PMMA (polymethyl-methacrylate) interfaces. Crack growth was measured under both cyclic and constant loading as a function of the applied G and relative humidity. The interface involving epoxy/PMMA differs significantly from those involving epoxy/glass or epoxy acrylate/glass since both epoxy and PMMA have low surface free energies [10] and, consequently, moisture would not be expected to be attracted to the crack tip at the epoxy/PMMA interface [10]. Thus, crack growth results at epoxy/PMMA interfaces should be less sensitive to humidity.

EXPERIMENTAL PROCEDURE

Crack growth under both constant and cyclic loading was studied using the interfacial, four-point flexure sandwich specimen, see Figure 1 [1,7,9]. The glass sandwich specimens consisted of two glass plates (40 by 8 by 1 mm) bonded together with an epoxy acrylate adhesive (50-008 DSM Desotech, Inc.) or an epoxy adhesive ("Two-Ton", Devcon Corp.). The PMMA sandwich specimens consisted of a top glass plate (40 by 8 by 1 mm) bonded to a bottom PMMA (OPTIX, Plaskolite Inc.) plate (40 by 8 by 2.25 mm) with an epoxy adhesive ("Two-Ton", Devcon Corp.). All specimens were made by pressing the top and bottom plates between two stops that were set to control the thickness of the interlayer to $30 \mu\text{m} \pm 15 \mu\text{m}$. Following the manufacturers' recommendations, the

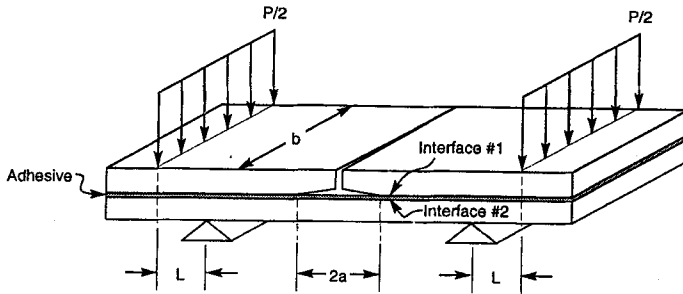


FIGURE 1 Schematic of the interfacial, four-point flexure sandwich specimen.

epoxy acrylate adhesive was cured for 24 h under ultraviolet light and the epoxy adhesive for 24 h in ambient air. After curing, the edges of the specimens were polished with 240 grit SiC abrasive paper to eliminate any excess adhesive that had squeezed out between the plates.

Precracking was achieved by placing several Vickers indentation cracks (indent load = 30 N) along the width of the top glass plate. Upon loading the sample in three-point bending with the indented surface on the tensile side, a crack propagated down from the array of indents to interface #1. For the epoxy acrylate/glass and epoxy/glass specimens, interfacial crack formation and growth were confined to interface #1, as shown in Figure 1, by abrading (mean surface roughness about 3 μm) the glass plate used at interface #2. The roughened glass surface at interface #2 increased the fracture resistance of this interface sufficiently so that crack formation and growth at this interface was inhibited [9]. For the epoxy/PMMA specimens, interfacial crack formation and growth were confined to interface #2 by using abraded glass at interface #1. However, the initial precrack in the top glass plate penetrated through the epoxy adhesive and into interface #2 in about one-half the specimens. In the other half of the specimens, the initial precrack arrested at interface #1 and a crack then formed on interface #2 with the epoxy adhesive remaining intact.

Crack growth under constant loading was monitored *in-situ* by constructing the four-point flexure apparatus to fit on the stage of an inverted optical microscope (Zeiss IM35), as shown schematically in Figure 2 [9]. The inner and outer spans were 22.23 and 31.75 mm, respectively. A button load cell (Sensotec Model 53) was used in conjunction with a digital

multimeter (Keithley 175) to record the applied load. The load was applied to the specimen by turning the micrometer. To maintain constant load, the micrometer screw had to be adjusted periodically. Crack growth in these experiments was monitored continuously with the microscope. The position of the interfacial crack was associated with interference fringes that were easily observable through the microscope. To measure the critical energy release rate, G_c , in this apparatus, the load was continuously increased until the interfacial crack propagated catastrophically. This caused the crack to go quickly out of the field of view in the microscope. Note that this apparatus was also used to precrack the specimens in three-point bending.

For cyclic loading, a four-point flexure fixture was constructed with dimensions similar to the constant load fixture (Fig. 2) and was used in conjunction with a servo-hydraulic Instron (Model 1321) that applied a sinusoidal load with a frequency of 3 Hz. Because of the limitation in the sensitivity of the load cell, the minimum load was set at about 9 N. For the glass sandwich specimens, this resulted in a ratio of minimum to maximum load of $R = 0.04$ to 0.50. Preliminary testing

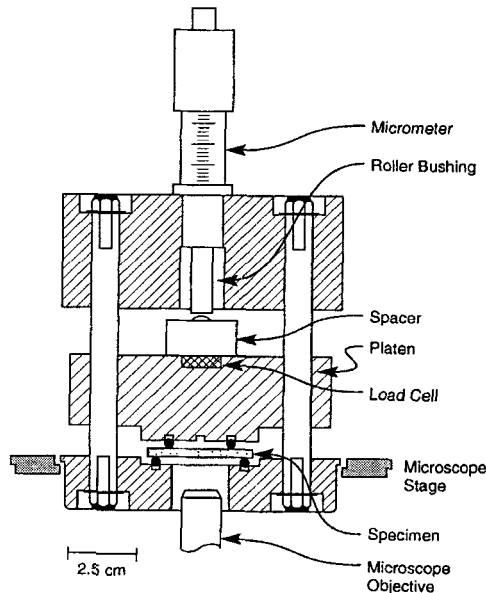


FIGURE 2 Schematic of the interfacial, four-point flexure apparatus for constant loading.

indicated that this load ratio range did not have a significant effect on the crack growth rate. For the PMMA sandwich specimens the load ratio varied from 0.04 to 0.14. Crack growth was monitored by interrupting the test periodically and measuring the crack length using the microscopic set-up for constant loading, Figure 2. To verify that the interrupted cycling between measurements did not affect the crack growth behavior, the number of cycles between interruptions and the time between sets of cycles were varied. Since the crack growth rate did not vary in a consistent way, it is assumed that the interrupted nature of loading had a negligible effect on crack growth behavior. In addition, crack growth in a few constant load tests was measured by interrupting the test. The crack growth rates measured by these interrupted tests were similar to those measured *in-situ*, again showing that interrupting the test did not influence the crack growth behavior. It should be noted that all crack fronts were relatively smooth across the width of the specimen and crack length was determined from several measurements along the crack front.

All crack growth experiments were carried out at either low (10–20% RH) or high (75–95% RH) humidity by enclosing the test fixture in a plastic envelope and then piping dry or moisture-saturated nitrogen gas into the envelope. Before testing, the specimens were preconditioned for 24 h in a bell jar maintained at the test humidity. This was done to ensure that each specimen was equilibrated to the test humidity before being placed in the test fixture.

For an applied load, P , and a thin adhesive layer, the energy release rate, G_o , for a crack on interface #1 can be derived based on a bi-material specimen to be [11]:

$$G_o = \frac{(PL)^2}{8b} \left(\frac{1}{E_2 I_2} - \frac{1}{E_c I_c} \right) \quad (1)$$

where b is the width of the specimen, L is the distance between inner and outer supports, I_2 is the moment of inertia of the bottom plate, $E_c I_c = E_1 I_1 + E_2 I_2$, E_i is the elastic modulus of plate i and I_i is the moment of inertia of plate i about the neutral axis of the composite beam. Finite element analysis (FEA) was carried out for the three crack geometries used in this study using the ABAQUS finite element program (Hibbitt, Karlson, and Sorenson, Inc.), and the results compared

with Eq. (1). The elastic moduli of glass and PMMA were taken to be 70 and 3.5 GPa, respectively, and the modulus of the polymer adhesive was taken as 2.8 GPa. Poisson's ratio for all 3 materials was assumed to be 0.3. The dimensions of the finite element model were taken to be the same as the test apparatus and sample dimensions were the same as the test specimens. The reader is referred to Ref. 9 for additional details of the finite element analysis.

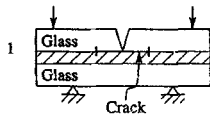
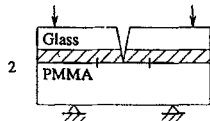
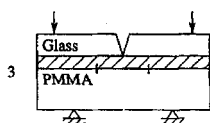
Table I summarizes these FEA results where G_{FEA} is the energy release rate determined from finite element analysis and G_o is the energy release rate calculated from Eq. (1). For cases 1 and 2, Table I shows that Eq. (1) agrees well with FEA, indicating that all of the strain energy in the specimen above the interfacial crack is relaxed. Since Eq. (1) does not include the relaxation in the adhesive layer, G_{FEA}/G_o for case 2 is 1.05. For case 3, FEA shows that because of the intact polymer adhesive, only a portion of the energy in the beam above the interfacial crack is relaxed. Also included in Table I is the phase angle ψ (a measure of the shear to tensile stress at the crack tip) for each of the crack geometries. Note that the characteristic length chosen for the calculation of the phase angle was the thickness of the adhesive layer. All these finite element results were essentially independent of the adhesive thickness from 20 to 80 μm and of interfacial crack length from $a = 1.0$ to 4.75 mm. Based on these FEA results, the appropriate G for a given crack geometry was calculated by multiplying G_o from Eq. (1) by the ratio given in Table I.

RESULTS

By carefully prying apart a sample after testing, both scanning electron microscopy (SEM) and X-ray photoelectron spectroscopy (XPS) of the crack surfaces could be carried out. Under both constant and cyclic loading, crack growth in all specimens was confined to the interface as both SEM and XPS of the surfaces revealed only polymer adhesive on one surface and either glass or PMMA on the other surface, depending on the specimen tested. Also, with the cyclic fatigue specimens no fatigue striations could be observed on any of the fracture surfaces.

Figure 3 compares constant loading crack growth along an epoxy acrylate/glass interface with that for cyclic loading on the same speci-

TABLE I Finite Element analysis results for the different crack geometries

Specimen	G_{FEA}/G_o	Ψ
	1.00	30°
	1.05	66°
	0.23	5°

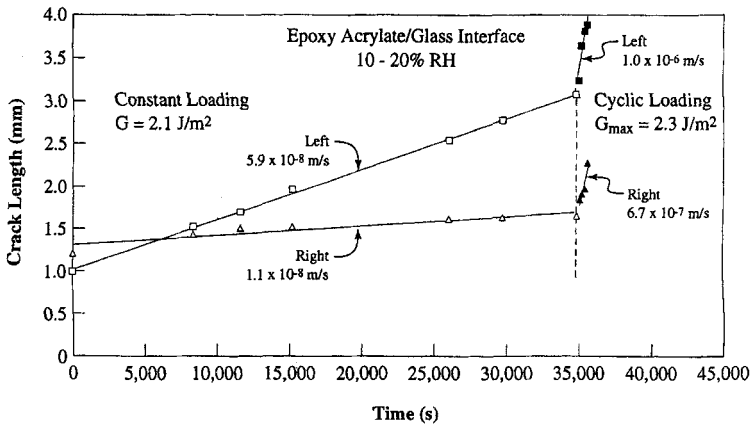


FIGURE 3 Comparison of crack growth along an epoxy acrylate/glass interface under constant and cyclic loading at 10–20% RH.

men at a test humidity of 10–20% RH. The straight lines labeled left and right refer to the crack growing on the left and right hand sides, respectively, of the specimen. To expedite such comparisons, the data in Figure 3 used G_{\max} in the cyclic loading as equivalent to G for constant loading and the number of loading cycles were converted to

humidity for the threshold energy release rate ($G_{th} = 0.30 \pm 0.06 \text{ J/m}^2$) under constant loading and the critical energy release rate ($G_c = 6.0 \pm 0.5 \text{ J}^2$). At the G_{th} no crack growth was observed in the time span of the experiment (up to 64 h). Note that the crack growth data are bracketed by these two values of G .

Our previous research has shown that crack growth rates at the epoxy acrylate/glass interface under constant loading at high humidity are significantly greater (about two orders of magnitude) than under low humidity [6, 7, 8]. On the other hand however, our present research shows that humidity has no effect on crack growth under cyclic loading. Figure 5 compares the crack velocities obtained under cyclic loading at high and low humidities. Also shown in Figure 5 are the data for constant loading at high humidity. The best fit line shown in the figure is that from the cyclic, low humidity data of Figure 4. It is evident from the data for cyclic loading in Figure 5 that humidity has no influence on crack growth rates under cyclic loading. As before, the arrows in Figure 5 represent the average G_{th} ($0.28 \pm 0.16 \text{ J/m}^2$) under constant load and G_c ($4.8 \pm 1.8 \text{ J/m}^2$), both measured under high humidity. By

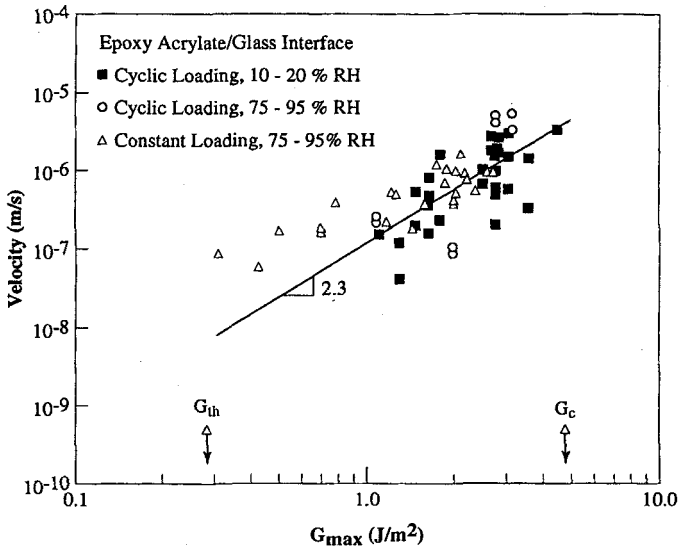


FIGURE 5 Comparison of crack growth rates on epoxy acrylate/glass interfaces under cyclic loading at 10–20% and 75–95% RH, and constant loading at 75–95% RH.

comparison with Figure 4, humidity has a small, perhaps negligible, effect on both G_{th} and G_c . Finally, it should be noted that, for clarity, not all the crack growth rates obtained at high humidity under cyclic and constant loading are included in Figure 5 since the data lie on top of one another. This is illustrated in Figure 6 where it is shown that crack growth rates at 75–95% RH for constant loading are about the same as those for cyclic loading at 10–20% RH on the same specimen.

Figure 7 compares the crack growth rates for epoxy/glass interfaces obtained under constant and cyclic loading at high and low humidities. Although crack growth was observed for all specimens tested at high humidity under constant load, it was very difficult to get crack growth in specimens tested at low humidity under constant load. Note that rather than give the average G_{th} for these low humidity data, all the data points with an arrow are for the samples that exhibited no crack growth. It is evident from the data that cyclic loading at low humidity enhanced crack growth substantially. The best fit line through the data ($V = 2.4 \times 10^{-8} G_{max}^{1.9}$, correlation coefficient = 0.61) is for the cyclic, low humidity data. Also indicated by arrows in Figure 7 are the average G_c obtained at low ($7.4 \pm 2.9 \text{ J/m}^2$) and high ($8.5 \pm 3.5 \text{ J/m}^2$) humidity, as well as the average G_{th} for constant loading at high humidity ($0.38 \pm 0.2 \text{ J/m}^2$). Similar to the epoxy acrylate/glass data, it does not appear that G_c is very sensitive to humidity within experimental scatter.

It is important to note the high experimental scatter (about an order of magnitude) that was observed both on the same sample (Fig. 3) and between multiple specimens (Figs. 4, 5, and 7). Other researchers have also seen this relatively high variability in fatigue crack growth at bi-material interfaces. For example, Jethwa and Kinloch [12] found that the standard deviation in fatigue crack growth rates at an epoxy/aluminum interface was about an order of magnitude. McNaney, Cannon, and Ritchie [13] showed that the variability in fatigue crack growth rates at aluminum/alumina interfaces were considerably greater than in either of the bulk materials. The variability in Figures 4, 5, and 7 can be attributed in part to the use of multiple specimens in determining the fatigue crack growth behavior. Also, contributions to this variability would be expected from the microstructural variability in the polymer adhesive and the extent of interfacial bonding.

Crack growth rates under constant loading at the epoxy/PMMA interface for both crack geometries studied (specimens 2 and 3 in

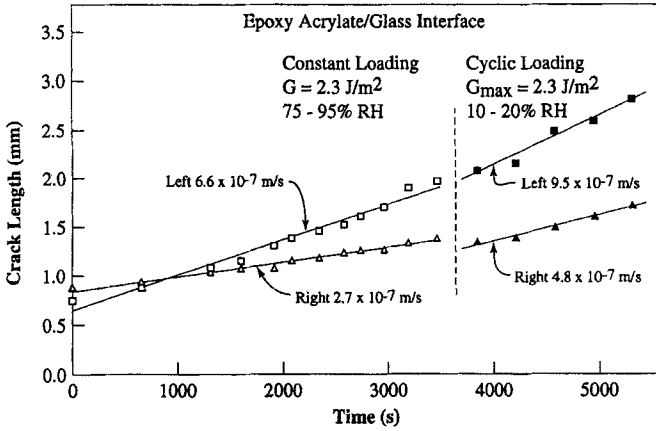


FIGURE 6 Comparison of crack growth rates along an epoxy acrylate/glass interface under constant loading at 75–95% RH with that under cyclic loading at 10–20% RH. The average measured G_{th} (constant load) and G_c values at 75–95% RH are indicated with arrows.

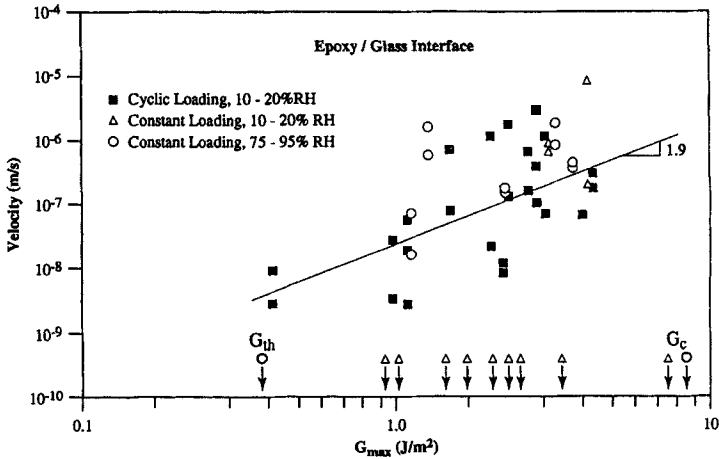


FIGURE 7 Comparison of crack growth rates along epoxy/glass interfaces under constant loading at 75–95% RH and 10–20% RH and cyclic loading at 10–20% RH. The data points with the arrows represent constant samples under constant loading and 10–20% RH that did not exhibit crack growth. The arrow besides the G_{th} value represents the average value measured for this quantity under constant load and 75–95% RH and the arrows besides the G_c values represent the average values measured at 10–20 and 75–95% RH, respectively.

Tab. I) were independent within experimental scatter of relative humidity (10 to 95% RH) of the test environment. Therefore, all the data were combined independent of test humidity and Figure 8 summarizes this data for both crack geometries.

Similar to the data for epoxy acrylate and epoxy/glass interfaces, *e.g.* Figures 4 and 7, it can be seen that all the crack growth rate data for a given specimen are bracketed between the G_c and G_{th} appropriate for that specimen. As before, these values of G_c and G_{th} are indicated by arrows. However, experimental scatter for crack growth rates on the epoxy/PMMA interface (about two orders of magnitude) is considerably greater than that observed for the epoxy acrylate and epoxy/glass interfaces (about one order of magnitude). It is possible that this large scatter seen with the use of multiple samples has masked any dependency of the crack growth rates on humidity or the applied G . However, it can be seen that it takes a significantly greater applied G to cause crack growth with specimen 2 ($\psi = 65^\circ$) than with specimen 3 ($\psi = 5^\circ$). This difference was also consistent with the measured critical energy release rates and threshold limits under constant load for the two crack

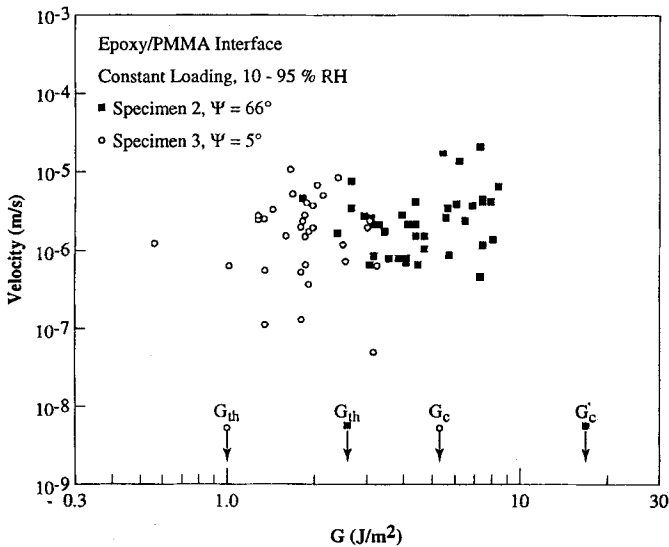
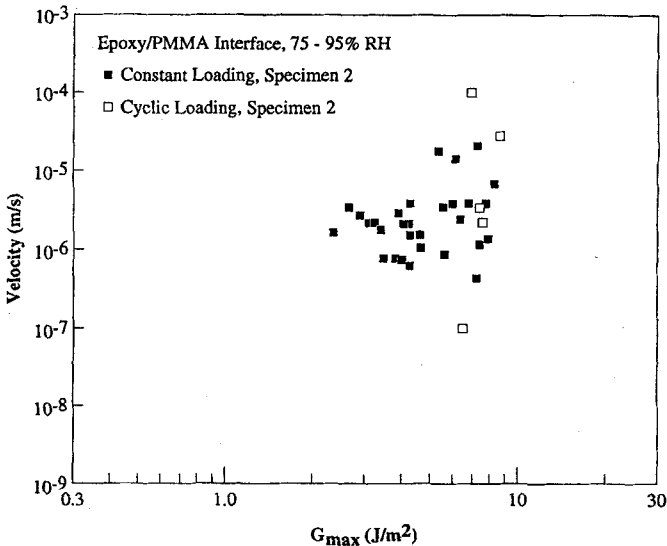


FIGURE 8 Crack growth rates along epoxy/PMMA interfaces under constant loading at 10–95% RH. The average measured G_{th} (constant load) and G_c values for specimen 2 and 3 are indicated with arrows.

geometries. For crack geometry 2, G_c was $17.9 \pm 7.3 \text{ J/m}^2$ and the threshold limit G_{th} was $2.5 \pm 1.4 \text{ J/m}^2$. For crack geometry 3, G_c was $5.2 \pm 2.4 \text{ J/m}^2$ and G_{th} was $1.0 \pm 0.56 \text{ J/m}^2$. These results indicate that crack growth under constant loading depends upon the phase angle at the crack tip. The more opening mode of loading at the crack tip in specimen 3 ($\psi = 5^\circ$) facilitates crack growth at applied G s less than those required for crack growth in specimen 2 ($\psi = 66^\circ$).

Figures 9a and b summarize the crack growth rates at the epoxy/PMMA interface under cyclic and constant loading at high humidity for the two different crack geometries. In an attempt to minimize the experimental scatter inherent in multiple sample testing, the data in Figure 9 were obtained by measuring on the same specimen the crack growth rate under constant and cyclic loading, similar to that shown in Figure 3. The result of this type of testing with both crack geometries was that there was no consistent crack growth pattern, *i.e.* sometimes constant loading gave a greater crack growth rate than cyclic and vice versa. For specimen 2 (Fig. 9a) the average crack growth rate under constant loading is $2.2 \times 10^{-6} \text{ m/s}$ and for cyclic loading $6.0 \times 10^{-6} \text{ m/s}$.



(a)

FIGURE 9 Comparison of crack growth rates along epoxy/PMMA interfaces under cyclic and constant loading at 75–95% RH for a) Specimen 2 and b) Specimen 3.

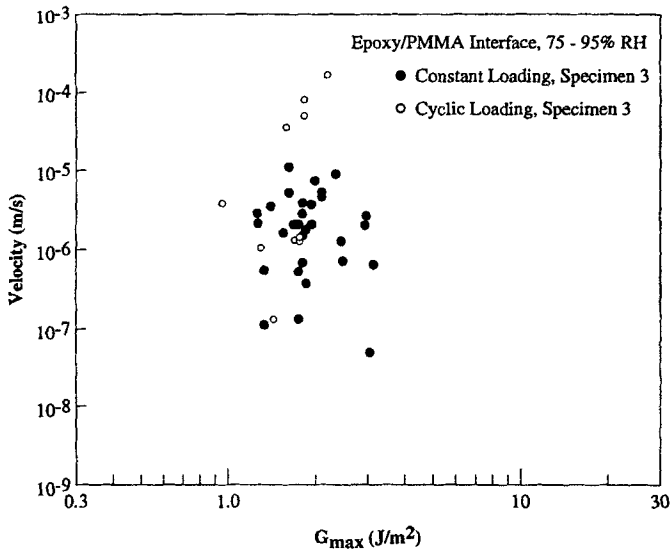


FIGURE 9 (Continued).

For specimen 3 (Fig. 9b) the average crack growth rate under constant loading is 1.6×10^{-6} m/s versus 3.1×10^{-6} m/s for cyclic loading. These epoxy/PMMA interface results are similar to those observed for epoxy acrylate/glass interfaces (Fig. 5) where, at high humidity, crack growth rates for constant and cyclic loading are similar.

DISCUSSION

The crack growth rate results involving the epoxy and epoxy acrylate/glass interfaces differ significantly from those involving the epoxy/PMMA interface. For the epoxy and epoxy acrylate/glass interfaces crack growth rates under both constant and cyclic loading fit a power law relationship ($V \propto G^n$), where the energy release rate exponent, n , is about 2.0. At low humidities, crack growth rates under cyclic loading are significantly greater than under constant loading; however, although high humidity enhanced crack growth rates under constant loading, high humidity had no effect on crack growth rates under cyclic loading. In addition, our previous research [9] showed that crack growth rates are

independent of phase angle from 13 to 55°, indicating that increasing shear at the interface does not cause a corresponding decrease in the fatigue crack growth rates at a given applied G . On the other hand, the crack growth rates for the epoxy/PMMA interface under both constant and cyclic loading are independent within experimental scatter of the applied G and relative humidity. Also, crack growth rates under constant and cyclic loading at all humidities are similar. However, the applied G to initiate fatigue crack growth at the epoxy/PMMA interface is considerably greater (about 2 to 3 times) for a phase angle of 66° than for 5°. Finally, it is important to realize that in all the polymer adhesive systems studied herein, no adhesion promoters were used; thus, the intrinsic adhesive bonding achieved in these systems is thought to be entirely due to van der Waals type bonding. This explains why crack growth was truly interfacial and the measured fracture toughnesses were relatively low.

In agreement with this study, Liechti and Chai [12] found that the fracture toughness, G_c , of an epoxy/glass interface was about 5 J/m² over a wide range of phase angles (about 0 to 70°). Note that the absolute value of the phase angle depends upon the choice of the length scale. Different values of the chosen length scale simply shift all phase angle values equally. Converting the phase angle of Liechti and Chai to our length scale (thickness of the adhesive layer) would shift their phase angle by about -20°. They proposed that the major contribution to the measured fracture toughness are:

$$G_c = \gamma_a + \dot{W}_p + \dot{W}_v + \Delta G_c \quad (2)$$

where γ_a is the intrinsic adhesive energy, \dot{W}_p is the rate of plastic dissipation per unit crack extension, \dot{W}_v is the rate of bulk viscoelastic dissipation per unit crack extension, and ΔG_c is the shielding effect due to the initial roughness of the interface. The possibility that microbranching of the main crack contributed to an increase in the overall toughness was not considered likely by Liechti and Chai because SEM micrographs of the epoxy fracture surfaces did not reveal any surface features. Careful SEM examinations of our crack surfaces also did not reveal any surface features, making it unlikely that microbranching could have occurred. Frictional contact of the crack surfaces and its effect on toughness was not considered by Liechti and Chai; but since the extent of crack face contact under some degree of

bond-normal applied displacements is expected to be less than $1\mu\text{m}$, this contribution was thought to be negligible.

The plastic dissipation contribution to the overall toughness was determined by Liechti and Chai [12] by numerically estimating the plastic zone in front of the crack tip. For moderate degrees of shear, they found \dot{W}_p to be constant with phase angle, similar to G_c , and equal to about 0.25 J/m^2 . The third contribution to G_c was determined by considering the viscoelastic dissipation in the bulk epoxy ahead of the crack tip for a loading-unloading cycle. Again, they found that \dot{W}_v was constant over moderate degrees of shear and equal to about 0.1 J/m^2 . The basic idea behind the surface roughness effect, ΔG_c , is that under some degree of shear, crack face asperities will interlock to provide a shielding, *i.e.* toughening, effect. However, since the glass surface is optically smooth, this effect for a moderate degree of shear is only about 10% of G_c [12]. Therefore, based on our measured value of G_c of about 8 J/m^2 for the epoxy/glass interface, the intrinsic adhesive energy can be found from Eq. (2) to be about 6.8 J/m^2 or 85% of the measured G_c . Note that Liechti and Chai estimated 4.0 J/m^2 for their epoxy/glass interface.

Assuming similar contributions of \dot{W}_p , \dot{W}_v and ΔG_c to G_c for the epoxy acrylate/glass interface, the intrinsic adhesive energy for the epoxy acrylate/glass interface (G_c about 5.5 J/m^2) is 4.6 J/m^2 . For the epoxy/PMMA interface (crack geometry 3, $\psi = 5^\circ$), it could be expected that the contributions of \dot{W}_p , \dot{W}_v , and ΔG_c to the interfacial toughness (5.2 J/m^2) would be similar to that of the epoxy/glass interface. This gives 4.3 J/m^2 for the intrinsic adhesive energy of the epoxy/PMMA interface. With crack geometry 2 ($\psi = 66^\circ$) of the epoxy/PMMA interface, considerable shear exists at the crack front that could cause a significant increase in both \dot{W}_p and \dot{W}_v . Based on $G_c = 17.9\text{ J/m}^2$, $\gamma_a = 4.3\text{ J/m}^2$, and $\Delta G_c = 0.1 G_c$, the plastic and viscoelastic contributions for specimen 2 can be estimated to be 11.8 J/m^2 . In this case it is likely that the plastic zone around the interfacial crack encompasses both the epoxy and PMMA.

In light of the above estimates of the contributions to the interfacial fracture toughness, it is of interest to assess quantitatively the extent of plasticity around the tip of an interfacial crack. For a crack at a bimaterial interface where the plastic zone is unconstrained, Shih [13] has shown that the crack tip plastic zone (r_p) in the lower yield

strength material (in this case the adhesive) is given by

$$r_p = \frac{\Lambda(E_1 E_2) G}{2\sigma_y^2(1 - \beta^2)(E_1 + E_2)} \quad (3)$$

where Λ is a constant equal to 0.15 for a phase angle of 0° and 0.70 for 90° , σ_y is the lower yield strength of the two materials across the interface, and β is a constant given by

$$\beta = \frac{1}{2} [\mu_1(1 - 2\nu_2) - \mu_2(1 - 2\nu_1)] / [\mu_1(1 - \nu_2) + \mu_2(1 - \nu_1)] \quad (4)$$

where μ_i is the shear modulus and ν_i is the Poisson's ratio of material i . All other terms have been previously defined. Table II summarizes the estimates of the "unconstrained" plastic zone in the adhesive layer for the different material combinations at $G = G_c$. The material properties used for these calculations are given in Table III where the moduli for the adhesives were determined from Hertzian indentation [14] and the yield strength estimated from the hardness ($\sigma_y = H/3.0$) [15]. Properties for glass and PMMA are handbook values and Poisson's ratio was assumed to be 0.3 for all materials. In all cases it can be seen that these "unconstrained" estimates of the plastic zone size are quite small relative to the adhesive thicknesses, and are consistent with our observations that no fatigue striations could be observed on the adhesive fracture surface and the relatively low estimate of \dot{W}_p . These estimates are also consistent with those estimated by Liechti and Chai [12] who found for moderate degrees of shear that the plastic zone size was less than $5 \mu\text{m}$ for a crack at an epoxy/glass interface.

SUMMARY

Based on the results of this research, it is believed that the mechanism of fatigue crack growth at epoxy and epoxy acrylate/glass interfaces differs substantially from that at epoxy/PMMA interfaces (see Fig. 10). For crack growth at a polymer adhesive interface with glass, the high surface free energy of the glass can attract water molecules to the crack tip [10]. These water molecules can then displace the polymer molecule

TABLE II Estimate of Plastic Zone Size at $G = G_c$

Material Pair	G_c (J/m^2)	r_p (μm)
Epoxy/Glass	8.0	0.4
Epoxy Acrylate/Glass	5.5	0.7
Epoxy/PMMA (Specimen 2)	17.9	0.90
Epoxy/PMMA (Specimen 3)	5.2	0.1

TABLE III Material Properties

Material	E (GPa)	μ (GPa)	σ_y (MPa)
Epoxy	3.0	1.15	65
Epoxy Acrylate	1.6	0.62	45
Glass	70	27.0	—
PMMA	3.5	1.35	—

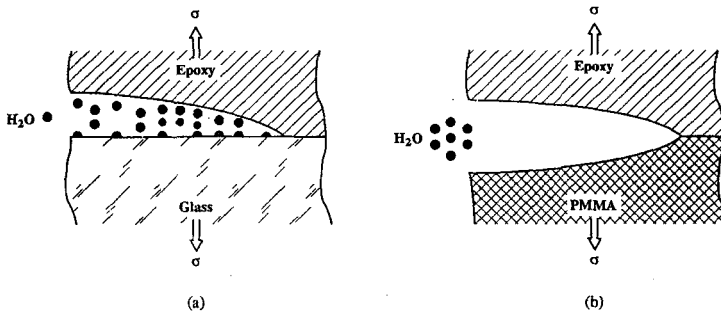


FIGURE 10 Schematic of the dependence on moisture of fatigue crack growth at a) epoxy/glass and b) epoxy/PMMA interfaces.

in the van der Waals bonding to the glass surface [16]. In terms of Eq. (2), γ_a is reduced by the presence of water [16]. As the applied G or relative humidity under constant load is increased, the crack tip becomes more accessible to moisture, thereby enhancing fatigue crack growth. Under cyclic loading the crack will try to close up on unloading and water will be trapped at the crack tip. This crack tip water can then act as a wedge to cause additional crack growth; however, based on the cyclic fatigue results, this wedging action of water at the crack tip is not very sensitive to the level of humidity in the test environment. Note that

similar explanations have been given for fatigue crack growth at mica interfaces [7, 18]. With the epoxy/PMMA interface, both crack surfaces are now low energy and water is not attracted to the crack tip [10]. Fatigue crack growth is now just a time-dependent separation that does not depend significantly, within experimental scatter, on the applied G , relative humidity, or cyclic vs. constant loading.

From an engineering design perspective, fatigue crack growth rates at polymer adhesive interfaces under either constant or cyclic loading can be characterized in terms of the energy release rate and test environment. However, variability in the crack propagation rates makes finite-life design predictions based on these rates too uncertain. Instead, we believe that adhesive joints subject to fatigue crack growth should be designed based on the fatigue threshold. The characterization of the fatigue threshold in terms of a probabilistic design framework is an area of future research.

Acknowledgment

This research was supported by NSF Grant DMR-9301761.

References

- [1] Cao, H. C. and Evans, A. G., "An Experimental Study of the Fracture Resistance of Bimaterial Interfaces," *Mech. Mater.* **7**, 295–304 (1989).
- [2] Suo, Z. and Hutchinson, J. W., "Sandwich Test Specimens for Measuring Interface Crack Toughness," *Mater. Sci. & Engr.* **A107**, 135–143 (1989).
- [3] Wang, J. S. and Suo, Z., "Experimental Determination of Interfacial Toughness Curves Using Brazil-Nut-Sandwiches," *Acta Metall. Mater.* **38**, 1279–1290 (1990).
- [4] Lai, Y.-H. and Dillard, D. A., "The Fracture Efficiency of Tests for Adhesive Bonds," to be published in *Int. J. Solids & Structures*, 1996.
- [5] Ritter, J. E., Grayeski, W. and Lardner, T. J., "Crack Propagation in Polymer/Glass Interfaces Under Monotonic and Cyclic Loading," pp. 245–250 in *Application of Fracture Mechanics in Electronic Packaging and Materials*, MD-Vol. 64, Wu, T. Y., Chen, W. T., Pearson, R. A. and Reid, D. T., Eds. (ASME, New York, 1995).
- [6] Ritter, J. E., Grayeski, W. and Lardner, T. J., "Cyclic Fatigue Crack Growth Along Polymer/Glass Interfaces," to be published in *Polym. Sci. & Engr.* 1996.
- [7] Conley, K. M., Ritter, J. E. and Lardner, T. J., "Subcritical Crack Growth Along Epoxy/Glass Interfaces," *J. Mater. Res.* **7**, 2621–2629 (1992).
- [8] Conley, K. M. and Ritter, J. E., "Moisture-Assisted Crack Propagation at Polymer/Glass Interfaces," *Int. J. Adhesion and Adhesives* **12**, 245–250 (1993).
- [9] Ritter, J. E., Lardner, T. J., Stewart, A. J. and Prakash, G. C., "Crack Propagation in Polymer Adhesive/Glass Sandwich Specimens," *J. Adhesion* **49**, 97–112 (1995).

- [10] Wu, S., *Polymer Interface and Adhesion* (Marcel Dekker, Inc., New York, 1982).
- [11] Charalambides, P. G., Lund, J., Evans, A. G. and McMeeking, R. M., "A Test Specimen for Determining Fracture Resistance of Bimaterial Interfaces," *J. Appl. Mech.* **56**, 77–82 (1989).
- [12] Jethwa, J. K. and Kinloch, A. J., "The Fatigue and Durability Behavior of Adhesive Systems for Automobile Applications", pp. 469–474 in *Proc. of the Fifth Annual Meeting of the Adhesion Society*, Ward, T. C., Ed. (The Adhesion Society, Blacksburg, VA, 1996).
- [13] McNaney, J. M., Cannon, R. M. and Ritchie, R. O., "Fracture and Fatigue Crack Growth Along Aluminum-Alumina Interfaces", to be published in *Acta Metall. Mater.*, 1996.
- [14] Liechti, K. M. and Chai, Y. S., "Asymmetric Shielding in Interfacial Fracture Under Inplane Shear," *ASME J. Appl. Mech.* **59**, 295–304 (1992).
- [15] Shih, C. F., Asaro, R. J. and O'Dowd, N. P., "Elastic-Plastic Analysis of Cracks on Bimaterial Interfaces: Part III-Large Scale Yielding," *J. Appl. Mech.* **58**, 450–463 (1991).
- [16] Ritter, J. E., Lardner, T. J., Rosenfeld, L. and Lin, M. R., "Measurement of Adhesion of Thin Polymer Coatings by Indentation," *J. Appl. Phys.* **66**, 3626–3634 (1989).
- [17] Ritter, J. E., Sioui, D. R. and Lardner, T. J., "Indentation Behavior of Polymer Coatings on Glass," *Polym. Eng. and Sci.* **32**, 1366–1371 (1992).
- [18] Kinloch, A. J., *Adhesion and Adhesives* (Chapman and Hall, New York, 1989).
- [19] Thomson, R., "The Molecular Wedge in a Brittle Crack: A Simulation of Mica/Water," *J. Mater. Res.* **5**, 524–534 (1990).
- [20] Wan, K.-T., "Fracture and Contact Adhesion Energies of Mica-Mica, Silica-Silica, and Mica-Silica Interfaces in Dry and Moist Atmospheres," *J. Am. Ceram. Soc.* **75**, 667–676 (1992).